DEMOCRATIC AND POPULAR ALGERIAN REPUBLIC
Ministry of Higher Education and Scientific Research
Saad Dahlab University-Blida1
Faculty of Sciences
Department of Physics

Master's Thesis in Medical Physics

Presented by: Mosuoe Bokang Molefi

Transition towards Non-Invasive Treatment for Cutaneous Carcinomas: Evaluation of 3D Dosimetry by Monte Carlo

JURY:

Mr. Djemai Bara	MRA	CDTA-Algiers	President
Mr. M.Laoues	MCB	USD-Blida1	Supervisor
Mr. A.SidiMoussa	Senior Medical Physicist	CSAC-Algiers	Examiner

Blida 2024

Abstract
Non-melanoma skin cancer (NMSC), comprising primarily basal cell carcinoma (BCC) and squamous cell carcinoma (SCC), is one of the most prevalent cancers globally, with its incidence rising annually. Traditional treatments, including surgical excision, cryosurgery, photodynamic therapy, and radiotherapy, have limitations such as potential for incomplete excision and cosmetic concerns. Superficial brachytherapy (SBT) with beta emissions from rhenium-188 (188Re) has emerged as a promising alternative. This study focuses on the dosimetric analysis of 188Re-based SBT using three-dimensional Monte Carlo GATE simulations to model the radiation dose distribution within treated tissues accurately. The primary objectives are to assess the safety, effectiveness, and potential clinical benefits of 188Re SBT in treating BCC and SCC. The research demonstrates that 188Re SBT achieves high treatment efficacy while minimizing impact on surrounding healthy tissues, thereby supporting its adoption as a standard therapy for NMSC and potentially improving patient outcomes and quality of life.
Keywords: Skin cancer treatment, Superficial brachytherapy (SBT), Rhenium-188 (188Re), GATE, Dosimetry.

Résumé
Le cancer de la peau non mélanomateux (CPNM), comprenant principalement le carcinome basocellulaire (CBC) et le carcinome épidermoïde (CE), est l'un des cancers les plus répandus dans le monde, avec une incidence en augmentation annuelle. Les traitements traditionnels, incluant l'excision chirurgicale, la cryochirurgie, la thérapie photodynamique et la radiothérapie, présentent des limites telles que le risque d'excision incomplète et des préoccupations esthétiques. La curiethérapie superficielle (CS) avec des émissions bêta de rhénium-188 (188Re) a émergé comme une alternative prometteuse. Cette étude se concentre sur l'analyse dosimétrique de la CS à base de 188Re en utilisant des simulations Monte Carlo tridimensionnelles GATE pour modéliser avec précision la distribution de la dose de radiation au sein des tissus traités. Les principaux objectifs sont d'évaluer la sécurité, l'efficacité et les bénéfices cliniques potentiels de la CS 188Re dans le traitement du CBC et du CE. La recherche démontre que la CS 188Re atteint une grande efficacité de traitement tout en minimisant l'impact sur les tissus sains environnants, soutenant ainsi son adoption comme thérapie standard pour le CPNM et améliorant potentiellement les résultats et la qualité de vie des patients.
Mots-clés : Traitement du cancer de la peau, Curiethérapie superficielle (CS), Rhénium-188 (188Re), GATE, Dosimétrie.

ملخص
سرطان الجلد غير الميلانيني (NMSC) ، والذي يتألف بشكل أساسي من سرطان الخلايا القاعدية (BCC) وسرطان الخلايا الحرشفية (SCC) ، هو واحد من أكثر أنواع السرطان انتشارًا على مستوى العالم، مع تزايد معدل الإصابة به سنويًا. العلاجات التقليدية، بما في ذلك الاستئصال الجراحي، الجراحة بالتجميد، العلاج الضوئي الديناميكي، والعلاج الإشعاعي، لديها قيود مثل احتمالية الاستئصال غير الكامل والمخاوف التجميلية. العلاج الإشعاعي الموضعي السطحي(SBT) بانبعاثات بيتا من الرينيوم-188 (188 Re) برز كبديل واعد. تركز هذه الدراسة على التحليل الجرعي لعلاج SBT المستند إلى 188 Reباستخدام محاكاة مونت كارلو ثلاثية الأبعاد GATE لنمذجة توزيع جرعة الإشعاع داخل الأنسجة المعالجة بدقة. الأهداف الرئيسية هي تقييم الأمان، الفعالية، والفوائد السريرية المحتملة لعلاج 188 Re SBTفي علاج BCC و .SCC تظهر الأبحاث أن علاج 188 Re SBT يحقق فعالية علاجية عالية مع تقليل التأثير على الأنسجة السليمة المحيطة، مما يدعم اعتماده كعلاج قياسي لسرطان الجلد غير الميلانيني NMSC وتحسين نتائج المرضى وجودة حياتهم بشكل محتمل.
الكلمات المفتاحية:علاج سرطان الجلد، العلاج الإشعاعي الموضعي السطحي(SBT) ، الرينيوم-188 (188 Re)، GATE،

Acknowledgements

I am profoundly thankful for the unwavering support and guidance of my advisor, Mr. M. Laoues, throughout my master's program. I thankful to Saad Dahlab university-Blida-1 for the resources that helped me complete this dissertation.

To my family, friends and classmates, your constant encouragement and support has been the cornerstone of this academic expedition. I am especially grateful to my mother for her unwavering support throughout my studies. This work stands as a testament to the collective support and contributions of everyone involved.

CONTENTS

LIST OF ABBREVIATIONS

SC-Skin cancer

NMSC-Non-melanoma skin cancer

BCC-Basal-cell carcinoma

SCC-Squamous-cell carcinoma

US-United States

UV-Ultraviolet

KSC-Keratinocyte skin cancer

CM-Cutaneous melanoma

PDT-Photodynamic therapy

PS-Photosensitiser

ED&C-Curettage and electrodesiccation

RT-Radiation therapy

EBRT-External beam radiation therapy

BT-Brachytherapy

SRT-Superficial radiation therapy

EBT-Electron beam Brachytherapy

LINAC-Linear Accelerator

MV-Mega voltage

HCl-Hydrochloric acid

IMQ-Imiquimod

5-FU-5-fluorouracil

EMA-European Medicines Agency

FDA-Food and Drug Administration

TLR7-Toll-like receptor 7

TLR8-Toll-like receptor 8

DNA-Deoxyribonucleic acid

D-Absorbed Dose

BSR-Superficial Brachytherapy though Radionuclides

SCT-Skin cancer

EPA- Environmental Protection Agency

ICRU-International Commission on Radiation Units & Measurement

LET-Linear Energy Transfer

BSR-Superficial Brachytherapy using Radionuclides

LIST OF FIGURES

LIST OF TABLES

GENERAL INTRODUCTION

Skin cancer, particularly non-melanoma skin cancer (NMSC), is one of the most prevalent forms of cancer worldwide, with its incidence steadily rising each year. NMSC primarily includes basal cell carcinoma (BCC) and squamous cell carcinoma (SCC), both of which originate from epidermal keratinocytes. While BCC is the most common and least aggressive type of skin cancer, SCC, though less common, has a higher potential for metastasis and mortality.

Traditional treatments for NMSC include surgical excision, cryosurgery, photodynamic therapy (PDT), and radiotherapy. However, these methods come with certain limitations such as potential for incomplete excision, cosmetic concerns, and in some cases, the need for highly specialized equipment and expertise. Among the various treatment modalities, superficial brachytherapy (SBT) with beta emissions, particularly utilizing rhenium-188 (188Re), has emerged as a promising alternative.

188Re is a radioisotope that emits beta particles with a relatively short half-life, making it suitable for targeting superficial lesions while minimizing exposure to deeper tissues and surrounding healthy structures. The application of 188Re in SBT involves the placement of the radioisotope close to or directly on the skin lesion, allowing for a highly localized dose of radiation that conforms to the shape of the tumor.

This thesis focuses on the dosimetric analysis of 188Re-based SBT, utilizing three-dimensional Monte Carlo GATE simulations to accurately model the radiation dose distribution within the treated tissues. The primary objectives are to assess the safety, effectiveness, and potential clinical benefits of 188Re SBT in the treatment of BCC and SCC. By providing a comprehensive evaluation of this novel treatment approach, this research aims to support its adoption as a standard therapy for NMSC, potentially improving patient outcomes and quality of life.

CHAPTER I: INTRODUCTION

I.1.SKIN CANCER

Skin cancer (SC) is one of the most common forms of cancer globally, especially among Caucasians and its cases continue to increase each passing year. The progression of skin cancer can happen due to many factors including direct exposure to UV radiation, skin colour, age, DNA damage, and many more. There are two main types of skin cancer which are Non-melanoma skin cancer (NMSC) or Keratinocyte skin cancer (KSC) and Melanoma skin cancer. Non-melanoma skin cancer is the most common type of Skin cancer and is further divided into basal cell carcinoma (BCC) and squamous cell carcinoma (SCC) [Leiter et al.2020;Hasan et al., 2023;Yélamos et al., 2023].

I.1.1. TYPES OF SKIN CANCER

I.1.1.A. MELANOMA SKIN CANCER

Melanoma skin cancer or cutaneous malignant carcinoma (CM) is a tumour that arises from epidermal melanocytes. CM, although less common than NMSC is the most deadly form of skin cancer and is prone to metastasis [Simões et al., 2015]. CM have a mortality rate of around 75%. However, CM is curable if detected early, with a cure rate of around 90% but it is difficult to treat once it has spread outside its original site. Although it can occur anywhere on the skin's surface, CM is often detected on the back for men and the lower legs for women [Simões et al., 2015;Naik et al., 2021;Orzan et al., 2015].

I.1.1.1.B. NON-MELANOMA SKIN CANCER

Non-melanoma skin cancers are the much more common than melanomas, but fortunately they are are less lethal than melanomas and are easier to treat and have better long-term prognosis. According to Globonan's estimations, there were 1,042,056 new cases of NMSC in 2018, and 65,155 deaths were attributed to NMSC(mostly SCC) [Hasan et al., 2023;Berwick et al., 2020]. NMSC is any other type of skin cancer that does not affect melanoma cells, with the most two most common forms being BCC and SCC of which both affect the epidermal keratinocytes, giving them the name Keratinocyte skin cancer(KSC) . Reports from the USA and Europe show that the rate of occurrence of NMSC is increasing each year [Leiter et al.2020;Hasan et al., 2023]. The assessment of the impact of BCC and SCC is difficult because most national tumour registries do not track them due to their large numbers [Berwick et al., 2020]. The major cause KSC is Ultraviolet (UV)

rays which is why they mostly progress in areas that are mostly such as the face and arms, making them one of the causes of disfigurement [Simões et al., 2015].

Basal cell carcinoma (BCC) is the most common type form of skin cancer in the world. Due to its low mortality rate, most cancer registries do not include data on BCC, however, BCC incidence is estimated to reach 4,3 million cases annually after analysing data from insurance registries and official statistics in the United States (US) [Dika et al., 2020]. BCC is slow-growing cancer that originates from the basal layer of the epidermis. BCC hardly ever metastasises to other parts of the body but it can expand to bones and nerves [Hasan et al., 2023;Linares et al., 2015]. BCC is mostly caused by exposure to UV rays hence it mostly affects areas that are directly exposed to sunlight such as the skin.

Squamous cell carcinoma (SCC) is the second most common form of SC and it a form of skin cancer with the second highest mortality. Over the last three decades, the number of SCCs has climbed from 50% to 300%, and by 2030, its frequency in European countries will have doubled [Corchado-Cobos et al., 2020]. SCC arises from the uncontrolled proliferation of epidermal keratinocytes. Although it usually exhibits benign clinical behaviour, it can spread locally and metastasise. Survival ten years after surgery is more than 90%, but it decreases significantly when metastases occur. The rate of lymph node metastases is about 4%, and the mortality is about 2% [Corchado-Cobos et al., 2020].

Figure I.1 show a representation different types skin cancer.

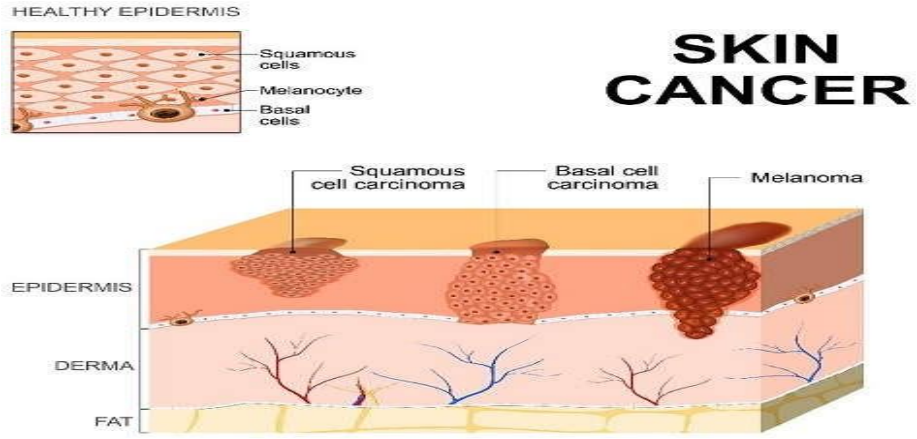

Figure I.1: Representation of basal cell carcinoma, squamous cell carcinoma and melanomas.

I.1.2. TREATMENT OF BASAL AND SQUAMOUS CELL CARCINOMA

Surgery is currently the main treatment for NMSC. In cases where surgery is impossible or not preferred, nonsurgical treatments including cryosurgery, curettage and electrodesiccation (or cautery), topical therapy, photodynamic therapy or radiotherapy can be used [Badash et al., 2019]

I.1.2.A. SURGERY

Surgery is a treatment in which the cancer cells are treated with a combination of chemotherapeutics and a partial removal of tissues with a use of surgical instruments. The aim of surgery is to remove the lesion along with a margin of healthy cells [Hasan et al., 2023;Badash et al.,2019]. There are different methods of surgery and they are as follows:

LOCAL EXCISION

In local surgical excision, the lesion is totally cut out along with some of the surrounding normal cells. The accepted surgical margins differ depending on the pathology, size of the tumour, location, and whether or not it is a primary or a recurring tumour. A major problem with local excision is that it can result an incomplete removal of the lesion because the definition of the tumour borders is often left to the surgeon's discretion [Anthony,2000].

MOHS MICROGRAPHIC SURGERY

Mohs microscopic surgery is the treatment choice for high risk NMSC and it offers high cure rates for NMSC. The surgery often used for recurrent type tumours and when tissue-sparring is needed. The surgery involves removing the tumour tissue. Once removed, the tumour tissue is then divided into sections and then it is marked with coloured dyes to facilitate the mapping of the surgical site. The tissue is then prepared and processed in the laboratory. The edges and undersurfaces of the sections are then analysed under a microscope. If cancer cells are detected, they are marked on the map and the corresponding tissue is removed from the patient. The process is repeated until cancer cell can longer be detected [Anthony,2000;Prickett et al., 2023].

The advantage of Mohs surgery is that it provides the patient with a high cure rate while it maximises the preservation of healthy tissue. The disadvantage are that the surgery takes a longtime because it is performed in many stages, and it needs a special laboratory and a specially trained surgeon [Anthony,2000]. Mohs surgery has 5-year cure rates especially for basal and squamous cell

carcinoma. This cure rates are: (99%) for primary BCC, (92-99%) for primary SCC, (94.4%) and (90%) for recurrent BCC and SCC respectively [Prickett et al., 2023].

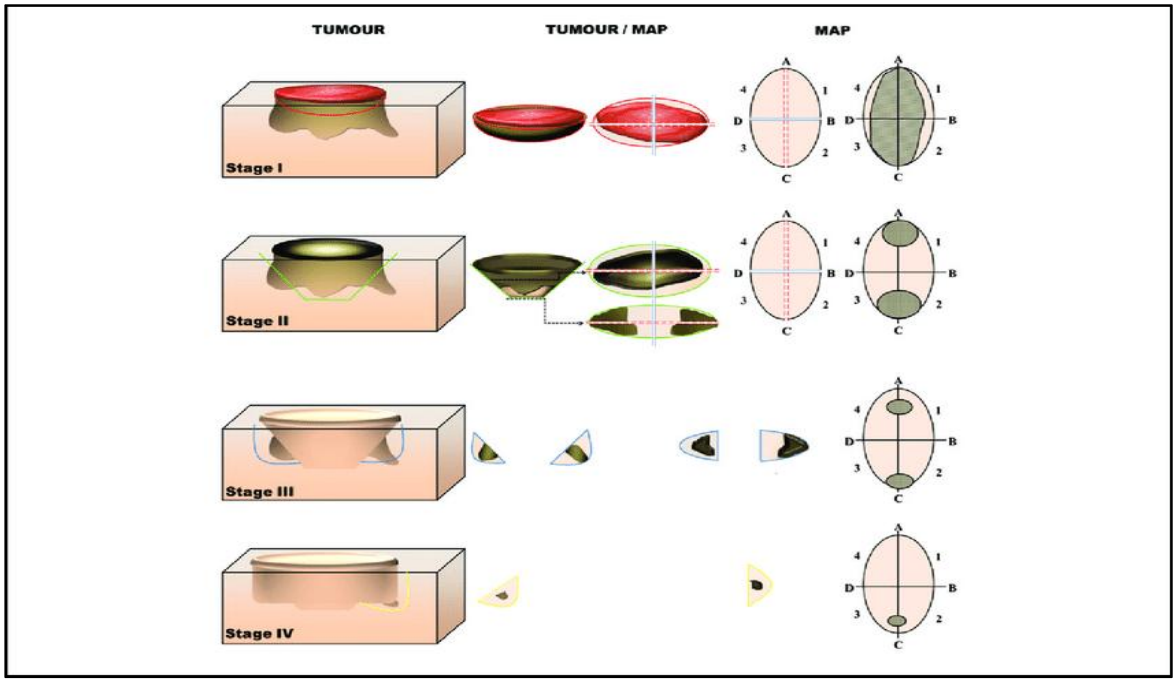

Figure I.2: Stages of Mohs micrographic surgery.

CURETTAGE AND ELECTRODESICCATION

Curettage and electrodesiccation (ED&C) is a technique that is used to treat small lesion that are on the upper part of the epidermis. The area to be removed is anaesthetised and the upper upper layer of lesion is removed used sharp spoon-shaped instrument called is a curette. After this, the wound is treated using mono-terminal electrode which destroys the remaining unhealthy cell and stops the bleeding. The process is repeated several time to achieve a complete removal of the tumour [Hasan et al., 2023;Anthony, 2000]. A study showed that a cure rate of (97-98%) after 5 year can be achieved for BCC. A study reported cure rates of 98.9% after 4 years for SCCs treated using ED&C [Fournier et al., 2020]. The advantages of this technique include a minute loss of blood, low cost, ease and convenience for patients. The disadvantages are that its success highly depends on the skill of the surgeon, if the surgeon is unskilled the is an increased risk of recurrence and that the treatment may leave a scar [Hasan et al., 2023;Anthony,2000].

I.1.2.B. PHOTODYNAMIC THERAPY

Photodynamic therapy (PDT) is a minimally invasive therapy that is based on activation of a photosensitive agent that is followed by a release of reactive oxygen species and tissue destruction. PDT treatment involves administrating of a photosensitiser molecule (PS) (topically and intravenous). The PS selectively accumulates in the tumour over a period of time. Tumour is subsequently exposed to light with an appropriated wavelength (generally in the red spectral region, ($\lambda \geq 600$ nm).This illumination and the presence of molecular oxygen causes a photodynamic reaction which begins with the absorption of light by the PS in the tumour which causes a series of photochemical reactions that lead to the generation of reactive oxygen species (ROS) such as singletoxygen ($^1O_2$), superoxide radical ($O_2^{-\bullet}$), hydroxyl radical ($HO^\bullet$) and hydrogen peroxide (H_2O_2). These radicals cause oxidative damage that can lead to cell death in the target tissue [Castellucci et al., 2021;Correia et al., 2021).

Photodynamic therapy has some advantages over conventional approaches to cancer treatment. Although some photosensitisers cause an increase in skin photosensitivity, it has no long-term side effects when used properly. It is less invasive than surgery and can be used for outpatients. PDT can be applied on the tumour accurately. There is little to no scarring after healing which leads good cosmetic outcomes. It can be applied on the same location several times. Some of its disadvantages are that it difficult to use for metastatic cancers. If not used correctly, it can lead to photosensitivity after treatment. The effectiveness of the treatment is dependent of on the amount of oxygen in the target tissue [Castellucci et al., 2021].

I.1.2.C. CRYOSURGERY

Cryosurgery (also known as cryotherapy or cryoablation) is a minimally invasive surgery treatment technique that is in alternative to surgical excision in older patients with multiple conditions that make them ineligible for surgery [Pustinsky et al., 2023]. Cryosurgery destroys tumours by using liquid nitrogen to reduce the tissue temperature to (-50 to 60° C) (freezing it). Multiple freeze-thaw cycles are recommended to increase the efficiency of the treatment [Linares et al., 2015].Contraindications to cryosurgery include tumours with indistinct margins, peri-neural or muscle invasion, involvement of bony structures, orbital tissues, and infiltrative advanced recurrent lesions, including relapses after radiotherapy [Pustinsky et al., 2023]. Cryosurgery is a simple, time-sparing, inexpensive and effective treatment for skin cancer. It offers optimal recovery for anatomical features and functions,as well as almost invisible and soft scars, resulting in good

cosmetic results. However, it can result in hypopigmentation, making it not preferable for darker skinned patients. Cryosurgery is only recommended when other treatment options are contraindicated or unfeasible since it does not get histological margin conformation [Pustinsky et al., 2023;Linares et al., 2015].

I.1.2.D. RADIOTHERAPY

Radiotherapy in an effective, adaptable, and easily accessible non-surgical treatment option for skin cancer. It is a tissue sparring technique that can, depending on the tumour and/or patient factors, be applied as external beam radiation therapy (EBRT) or as brachytherapy (BT). RT can be used as an alternative to surgery in cases where surgery may not be possible (Definitive radiotherapy) or as additional (adjuvant) treatment to kill the remaining unhealthy cells after surgery [Garbutcheon-Singh et al., 2019]. EBRT can be delivered with low energy photons (superficial radiation therapy), electrons (electron beam radiation therapy), or in rare cases with mega-voltage (MV) photons [Locke et al., 2001].

Superficial radiation therapy (SRT) uses low energy photons ar X-rays (in the the range of 50-150 kVp) to destroy the lesion by stopping mitosis, thereby stopping further cell division. A dose of 45 Gy is normally delivered in 3 Gy fractions. However, the dose to be delivered in SRT varies depending on the sizes of the tumour, patient, and/or whether or not they have any comorbidities [McGregor et al., 2015]. Electron Beam radiation therapy (EBT) is a treatment that targets superficial tumours by delivering a dose with 6-20 MeV electrons using a LINAC. EBT is used for tumours with depths of up to 5 cm. MV photons are used for advanced lesions, tumours with a deep-set component, or close to critical structures. Due to their high energies, MV photons donot deposit most of their energy on the skin therefore there is a need for a compensator (bolus) to beplaced on the tumour [Yosefof et al., 2023]

Brachytherapy is an alternative that uses radiation from decaying radioisotopes. The radioisotopes can be placed inside the tumour (interstitial brachytherapy) or close to the tumour (superficial brachytherapy). Brachytherapy enables treatment of lesions on the curvy parts of the body and near critical organs. It also permits treatment of large tumours while using the least amount of harm to healthy cells and has good cosmetic results [Skowronek,2015].

There exists multiple fractionation options for different types of tumour within RT, ranging from conventional fractionation (2 Gy per day) to extreme hypo-fractionation of up to 20 Gy per fraction [Zaorsky et al., 2017].

Hypo-fractionation can be beneficial for the elderly, poor performance patient where conventional fractionation may be difficult or inappropriate to deliver [Garbutcheon-Singh et al., 2019]. Results from 344 articles published between 1985-2016 showed that more than 80% of BCC/SCC patients had positive cosmetic results from hypo-fractionated RT [Hasan et al., 2023].

Figure I.3: a) above shows the lesion to be treated and below shows the treatment using superficial brachytherapy. b) LINAC with applicator for external beam radiation therapy usingelectrons.

I.1.2.E. TOPICAL TREATMENT

Topical treatments can be used in cases where surgery is rejected or not possible. Topical treatment may allow high doses to the tumour with lower toxicity to the patient [Kopera,2021]. Imiquimod (IMD) and 5-fluorouracil (5-FU) the two commonly used topical treatments.

IMIQUIMOD

Topical imiquimod through the use of the Food and Drug Administration (FDA) and European Medicines Agency (EMA) approved 5% IMQ cream has shown to be useful in treating NMSC while having insignificant effect to the skin [Gracia-Cazañaet al., 2016]. Imiquimod is a synthetic compound that belongs to the imidazoquinoline family. IMQ blocks the toll-like receptor7 (TLR7) and TLR8, triggering the body's innate and acquired immunity through the production and release of cytokines [Gross et al., 2007].

A publication analysing data from 100 diagnosed superficial BCC showed that 83.5% were disease-free one year after therapy and 5 years after therapy 85.5% of the patients showed no signs of recurrence [Kopera,2021]. IMD may cause local and systemic effects like redness, erosion, crusting,

blistering, pruritus, fatigue, flu-like symptoms, myalgia and headaches, which may, depending on the severity and medical intervention [Cullen et al., 2020].

5-FU

The FDA approved 5% cream or solution of 5-FU is a common agent used in the treatment of superficial BCC. The cream is applied twice a day for a duration of 2-4 weeks. 5-FU is an antineoplastic pyrimidine analog [Hasan et al., 2023]. It works by interfering with DNA synthesis by inhibiting thymidylate synthase and as a result inhibiting cell proliferation [Gross et al., 2007]. A clinical study evaluated 29 patients (with 31 superficial BCC lesions) showed 90% histologic cure rate which is comparable with other treatment options. The study also showed that the treatment has good cosmetic results and a high patient satisfaction [Gross et al., 2007]. The noticeable side effects of %-FU are lysis of blood, hair loss, erythema, oedema and sever local skin eruptions [Sahu et al., 2019].

I.3. THE NEED FOR NON-INVASIVE TREATMENT

These are some of the reason we need non-invasive cancer treatment modalities.

- Preservation of healthy tissue: Non-invasive treatments such as brachytherapy allow treatment of tumours while causing little to no harm to healthy cells [Skowronek, 2015].
- Accessibility: Non-invasive treatments such as cryosurgery provide an alternative treatment to patients who are not eligible for surgical treatment due to multiple health reasons for those who refuse to have surgery [Pustinsky et al., 2023].
- Allows combination of therapies: Non-invasive treatments can be used together with surgery or each other in order to improve results [Fournier et al., 2020;Garbutcheon. S et al., 2019].
- Improved outcomes: Non-invasive are tissue-sparring allowing for better cosmetic outcomes and some have high cure rates [Pustinsky et al., 2023].
- Convenience: Many non-invasive treatments are done on outpatient basis, meaning patients can return home right away after treatment without needing to be hospitalised[Castellucci et al., 2021]

I.4. RHENIUM-188

Rhenium-188 is high energy beta emitting radioisotope, with a 85% 2.1 MeV Beta radiation emission and 15% 155 keV gamma radiation emission. It has a physical half-life of 16.9 hours ($T_{½}$=16.9 h) and a maximum penetration of 11 mm. It deposits 92% of its energy within 2 mm depth in the skin. Its Therapeutic effect is up to 3 mm in depth making it most suitable for treating tumours that are less than 3 mm deep. ^{188}Re has flat dose distribution in depth hence it provides a homogeneous dose to the tumour [Castellucci et al., 2021;Cipriani et al., 2020;Lepareur et al., 2019]. ^{188}Re undergoes a beta decay and the product is Osmium (Os) as shown in figure I.4 [Pillai et al., 2012].

1.4.1. RHENIUM PRODUCTION

Rhenium-188 can be produced through the irradiation of natural rhenium in a reactor or in a ^{188}W/^{188}Re generator. The former yields a mixture of ^{186}Re and ^{188}Re, the proportion of each radioisotope depends on the irradiation time and post irradiation decay. Table 1 summarises the characteristics of ^{186}Re and ^{188}Re [Pillai et al., 2012]. This section section discusses the production of rhenium using the ^{188} W/^{188}Re generators. The ^{188}W/^{188}Re generator has a relatively rapid ^{188}Re daughter in-growth (~60% in 24 h) following bolus elution, allowing elution everyday, which makes itattractive for clinical use [Lepareur et al., 2019].

Table I: Decay characteristics and Production Methods of ^{186}Re and ^{188}Re.

	Decay Product	Half-life	β⁻ Emax(MeV)	γ-energy (keV)	Production
^{186}Re	^{186}W (EC, 7.47%) ^{186}Os(β⁻, 92.43%)	90 h	1.069 (71.0%) 0.932 (21.54%) 0.581 (5.78%) 0.459 (1.69%)	137 (9.42%)	^{185}Re(n,) ^{186}Re
^{188}Re	^{188}Os (β⁻, 100%)	17 h	2.120 (71.1%) 1.965 (25.6%) 1.487 (1.65%)	155 (15.1%)	^{188}W/^{188}Re generator or ^{187}Re(n,) ^{188}Re

^{188}W PRODUCTION

Tungsten-188 (^{166}W) is produced in reactor by double neutron capture of enriched tungsten-186 targets. Figure I.4 illustrates the schema of this reaction along with the decay schema of the reaction. ^{188}W has a half-life of 69 days making it suitable for uses in generator [Lepareur et al., 2019;Pillai et al., 2012]. Isotopically enriched ^{188}W (>90%) is used in the production of ^{188}W because neutron capture produces a variety of unwanted radioisotope products. High thermal neutron flux reactors with a thermal neutron flux of at least 10^{10} neutrons/cm^3 are required for the production of ^{188}W with a sufficient specific activity for generator use. A two-fold increase in the thermal neutron flux leads to double the ^{188W} product yield for the double neutron capture process [Lepareur et al., 2019].

The ^{188}W targets are processed, this processing involves high temperature conversion of the irradiated metallic ^{188}W/^{186}W with atmospheric oxygen using a quartz glass reaction apparatus. The resulting [^{188}W]WO_2 is subsequently dissolved by using caustic and provides ^{188}W-tungstate ([^{188}W]Na_2WO_4) stock solution which is then acidified with HCl into tungstic acid ([^{188}W]HWO_4) with pH 2-3. Only a small percentage of the ^{188}W is activated during irradiation, due to this, once the activity level of the eluted ^{188}Re-perrhenate equilibrium from the generator are to low for pharmaceutical preparation the remaining non activated ^{188}W on the generator matrix can be removed by elution and then reprocessed for activation [Lepareur et al., 2019].

^{188}W/^{188}Re GENERATOR

The ^{188}W/^{188}Re generator is similar to the ^{99}Mo/^{99}Tc generator. The generator comprises of a column containing ^{188}W which later decays into ^{188}Re as shown in Figure I.4 [Lepareur et al., 2019]. Different methods of separating ^{188}Re from ^{188}W have been developed but this paper discusses alumina-based generator [Pillai et al., 2012]. In an alumina-based generator the tungstic acid is slowly percolated through a saline-washed alumina column which then thoroughly washed with additional saline solution. The generator is slowly eluted saline to ensure the removal of the ^{188}Re bolus. The volume of saline depends on the generator size but is typically 1-2 ml/min. The automation or semi-automation of this process has helped move forward the use of the generator and allows result reproducibility and lesser radiation on personnel. The elution can be automated to only happen at peak in order to optimise the bolus ^{188}Re volume [Lepareur et al., 2019].

Due to low specific volume (Ci/ml) of ^{188}W, higher volumes of saline are required for elution of ^{188}Re eluents, resulting in low specific volumes. With high activity generators this not required. However, the use of of bolus concentration can help increase of the generator's shelf-life. Post-

elution concentration of the ^{188}Re bolus solution, which is based on a strategy which focuses on the separation of the eluent anions and subsequent trapping of the eluted ^{188}Re-perrhenate, is a convenient and useful way to extend the ^{188}W/^{188}Re generator half-life. The most commonly used method to do this involves a simple two tandem flow-through system based on the separation of the chloride anions (Cl^-) from the saline solution from the microscopiclevels of the eluted perrhenate anions ($[^{188}Re]ReO_4^-$).This done by passing the saline solution through silver-nitrate-based anion trapping column which traps the Cl^- while letting the perrhenate anions flow through and are in turn trapped in the second anions trapping column. The perrhenate is obtained from the second column by low level volume elution and a high Re specific volume solution is obtained. The ^{188}Re-perrhenate is then used to make pharmaceuticals [Lepareur et al., 2019].

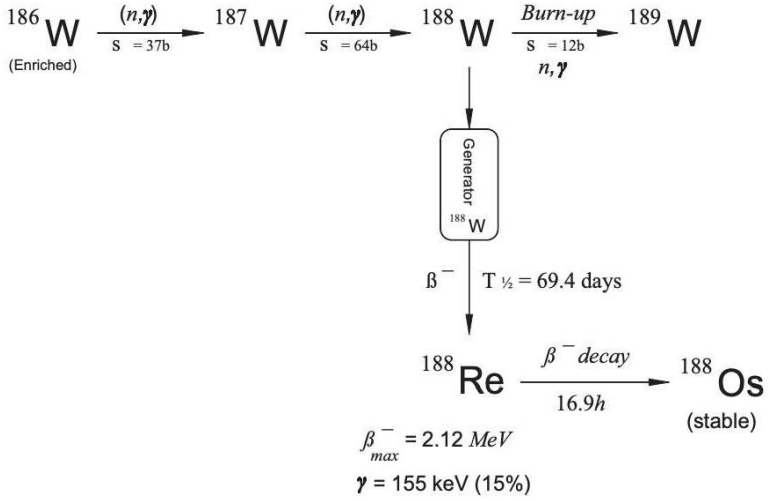

Figure I.4: Schema of tungsten-188 reactor production and decay.

1.4.2. TOPICAL TREATMENT USING RHENIUM-188

Among the many treatments for skin cancer, there exists topical treatment by means of radionuclides, also called Superficial Brachytherapy though Radionuclides (BSR). BSR is a treatment based on the application of radionuclides on the skin surface. (W. Rodríguez-Herklotz). There have been several cases of treating cancer with topical application of radionuclides that have been reported e.g using ^{125}I seeds on a gold plaque and using ^{166}Ho patch [Jeong et al., 2003] .Recently, a high dose brachytherapy technique using a non sealed rhenium-188 resin, known as Rhenium SCT® (Skin Cancer Therapy)(figure I.6) has emerged. In this treatment rhenium-188 is homogenously mixed in a cream and distributed on top of a plastic sheet to avoid the contamination of the skin (W. Rodríguez-Herklotz).Rhenium has become an important radionuclide for therapy

due to its physiochemical properties and ability to install generators (^{188}W/$^{!88}$Re-generators) in general hospitals [Jeong et al., 2003;Castellucci et al., 2021].

Brachytherapy with ^{188}Re may be used in cases where (a) other treatment approaches would not be inadequate with regard to location, the extend of the tumour or resultant cosmetic outcomes from surgery; (b) the patients have health conditions or comorbidities that can make them ineligible for surgery; and (c) patients who refusesurgery[Castellucci et al., 2021].^{188}Re's steep dose drop off after 3 mm allows to spare underlying tissue [Cipriani et al., 2020]. Brachytherapy with ^{188}Re (Rhenium SCT®) offers the possibility to treat several lesions at one and the possibility to treat almost every anatomical location. The technique has also proven to have good cosmetic results although some of the treated areas may show slight depigmentation of the skin and hair loss.[Rodriguez-Herklotz et al., 2022;Castellucci et al., 2021].

A study was conducted between October 2017 and January 2020, where patients affected by NMSC (including both new diagnosis and relapses) were selected by the Dermatologist Unit of the Azienda Ospedaliero-Universiteria of Bologna, S Orsola-Malphigi Hospital undergo treatment with Rhenium SCT®. The inclusion criteria for the study were (1) proven to have cutaneous BCC or SCC; (2) lesion thickness not deeper than 2.5 mm; (3) lesions located on the scalp, face, ears, or fingers or other areas in which other treatments modalities would have been to perform; (4) contraindications or the patient's refusal to surgery. 50 patients (15 female,35 male age range 56-93, mean age 81) diagnosed with 60 NMSC lesions(41 BCC, !8 SCC, 1 BCC&SCC) were enrolled for treatment. Of the 60 lesions, 18 had already been treated using other therapies and had relapsed, while 42 were newly diagnosed [Castellucci et al., 2021].

The mean time for the treatment was 79 minutes (range 21 to 285 minutes). The patients were examined by a dermatologist on days 14,30,60,90,180 after treatment and then every 90 to 180 days. The study concluded that high dose brachytherapy using a non sealed ^{188}Re resin is a non-invasive and easy to perform treatment. The trials showed that the therapy was effective in 98% of the treated population. The results from this trial show Rhenium SCT® has a potential to become a viable alternative to surgery [Castellucci et al., 2021].

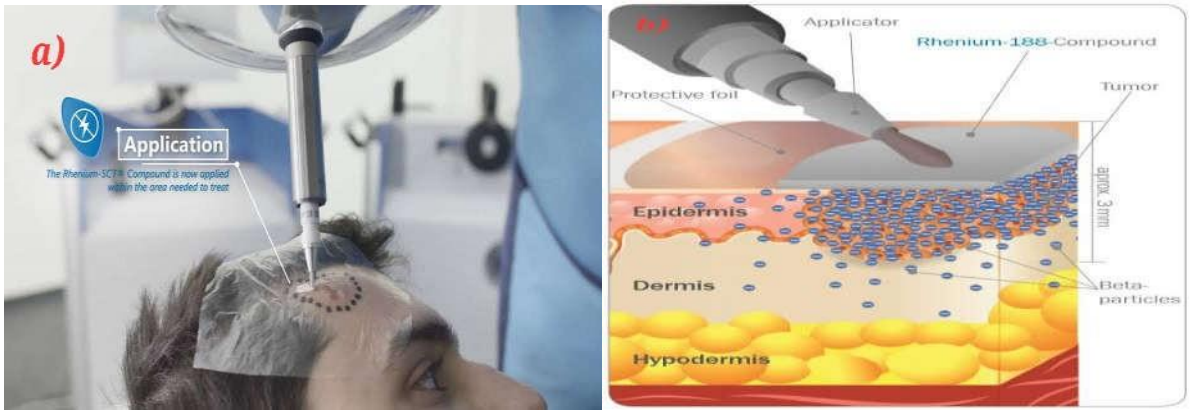

Figure I.5: (a) Rhenium-SCT compound being applied on the area to be treated. (B) Schematic representation of Rhenium-SCT.

I.5. LIMITATIONS TO THE 2D DESCRIPTION OF THE ABSORBED DOSE DISTRIBUTION

Before discussing the limitations we first have to define what the absorbed dose (D) is. According to the National Research Council (U.S) Committee on Evaluation of EPA Guidelines for Exposure to Naturally Occurring Radioactive Materials, the absorbed dose (D) refers to the energy imparted by radiation per unit mass of irradiated material. Absorbed dose is expressed in rad or in Gray (Gy) [NRC] .

Limitations of two-dimensional dose descriptions are that they only report the average doses at the maximum lesion depth, averages over the entire volume, and the averages at the surface without showing information of the homogeneity in the dose distribution. The other limit is that the dose distribution to healthy cells cannot be calculated [Rodriguez-Herklotz et al, 2022].

CHAPTER II: THE MONTE CARLO GATE SIMULATION PLATFORM FOR DOSIMETRIC APPLICATIONS

INTRODUCTION

When an incident particle traverses matter, it passes near electrons or atomic nuclei with which it can interact. The type of interaction depends on the nature of the particle, its energy, and the surrounding medium. Simulating the trajectory of this particle involves reproducing its behaviour in the medium while accounting for these interactions. The Monte Carlo method is particularly well- suited to this constraint as it provides a valuable tool for optimizing energy deposits and calculating dose distributions efficiently and accurately. Several codes have been developed or adapted for medical applications (see the first chapter). The performance and effectiveness of these codes result from the implementation of physical processes based on effective cross-section libraries.

To introduce the treatment of ocular melanomas using brachytherapy with ophthalmic applicators in Algeria, we focused on validating the Monte Carlo GATE (Geant4 Application for Tomographic Emission) simulation platform for dosimetric applications using electrons. GATE is a simulation tool dedicated to medical physics applications, based on the Monte Carlo GEANT4 code originally developed for high-energy physics. One of the objectives of this thesis is to validate the physical processes of the GATE platform for dosimetric applications using electrons to enable its future use in ocular treatment planning.

Several studies have been conducted with GATE [Jan et al., 2004; Maigne, 2005; Sarrut et al., 2014] to make this simulation tool more efficient and user-friendly with acceptable computation times. The first part will be devoted to the GEANT4 code, explaining the various physical processes involved in energy deposition and their implementation. We will focus particularly on the simulation of electron transport in GEANT4. The second part will detail the use of the GATE platform and its various functionalities, especially for dosimetric applications.

II.1 ELECTROMAGNETIC PROCESSES IN GEANT4

II.1.1 INTERACTIONS OF ELECTRONS IN MEDICAL PHYSICS

II.1.1.A IONIZATION

When an electron passes through a medium, it undergoes Coulomb interactions (collisions) with electrons in the medium. These interactions cause an energy loss (Q) ranging from 0 (distant collision) to T (head-on collision). The incident electron retains the highest kinetic energy after the collision; the energy transfer (Q) to the target electron has a maximum value of T/2. Distant collisions are more frequent than close collisions: the electron loses its energy (T) primarily throughnumerous small transfers. Over a short path length Δx, the electron's energy (T) exhibits statistical fluctuations around an average value ΔT. The stopping power or linear energy transfer (LET by collision) of the medium concerning electrons with energy (T) is defined by Equation II.1 [Blanc, 1997].

$$TEL_{col} = \frac{\Delta T}{\Delta x} \quad \textbf{\textit{Equation II.1}}$$

It is expressed in MeV/cm and characterizes the electron's deceleration (depending on the energy (T) and the medium). This value can be calculated using the Bethe-Bloch formula [Blanc, 1997]. The average energy loss per collision (ionizations and excitations) is given by the simplified relativistic Bethe-Bloch formula for the non-relativistic electron kinetic energies (Equation II.2).

$$\frac{dE}{dx} = 0.15\frac{Z}{A\beta^2} ln\left[\frac{\alpha^2(\alpha+2)}{2\mathfrak{I}c^2}\right] \quad \textbf{\textit{Equation II.2}}$$

with $\alpha = E0/mc^2$ et $\beta = \alpha\,(\alpha+2)/(\alpha+1)$

A is the atomic mass and Z is the atomic number of the medium. I denotes the mean excitation potential of the medium and is expressed as: $I = 18.35Z^{0.835}$

II.1.1.B BREMSSTRAHLUNG

The interaction of the incident electron with the target nucleus results in a change in the electron's direction, i.e., scattering accompanied by the emission of radiation (photon) with energy (E) taken from the electron's kinetic energy (T). The electron is thus decelerated, and its energy is reduced to (T-E). This interaction is known as "braking" and the emitted radiation is "bremsstrahlung" or "braking radiation." Due to the considerable mass difference, the energy transfer (Q) is practically negligible (Equation II.3)

$$Q_{max} = 4\frac{m}{m'}T \quad \textbf{\textit{Equation II.3}}$$

with $m' << m$.

The average energy lost by an electron with energy (T) through "braking" over a segment Δx of its trajectory is ΔTr (sum of the energies of the emitted photons). The stopping power or linear energy transfer by braking is defined by:

$$TEL_f = \frac{\Delta T_r}{\Delta x} \quad \textit{Equation II.4}$$

It is calculated using the simplified relativistic Bethe-Bloch formula for the non-relativistic electron kinetic energies (Equation II.5).

$$-\frac{dE}{dx} = \frac{NEZ(Z+1)e^4}{137(mc^2)^2}\left[4ln\frac{2E}{mc^2} - \frac{4}{3}\right] \quad \textit{Equation II.5}$$

The total stopping power is defined by the total energy loss resulting from collisions and braking:

$$TEL = TEL_{col} + TEL_f$$

The bremsstrahlung interaction is significant only for very high-energy electrons (> 10 MeV). The medium also influences the type of collision. Energy loss due to braking radiation emission is proportional to Z2, while loss due to collision is proportional to Z. Therefore, heavy elements produce a much greater loss by braking radiation (see Figure II.1).

For low energies, collision energy loss predominates, and we observe an overlap between the stopping power by collision and the total stopping power. The ratio of radiative to collision energyloss is approximated as follows:

$$\frac{(dE/dx)_{rad}}{(dE/dx)_{col}} \approx \frac{EZ}{700} \quad \textit{Equation II.6}$$

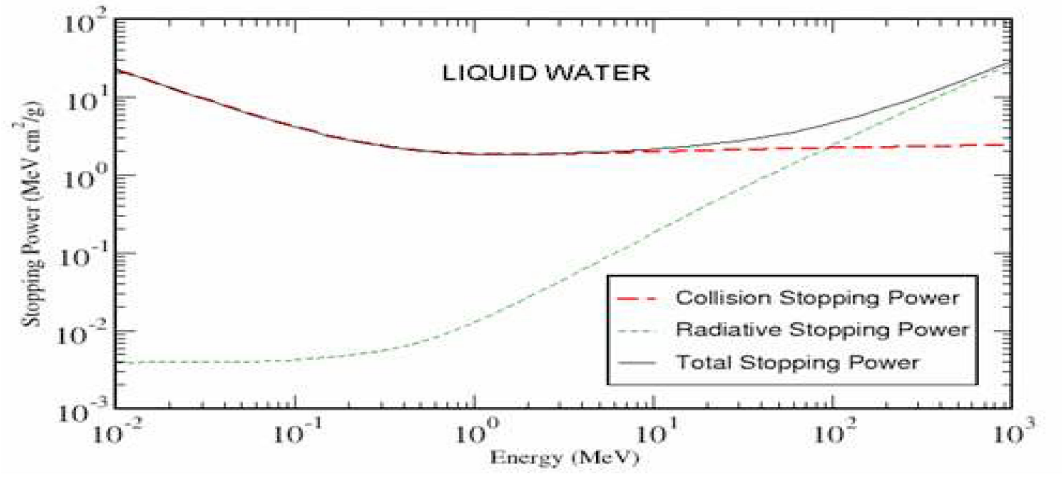

Figure II.1: Energy loss by collision or radiation of electrons in liquid water.

II.1.2 ELECTRON PATHS: PENETRATION DEPTH

An electron with initial energy E0 gradually loses its energy as it traverses a medium, with its trajectory ending when its energy becomes practically zero. Since the electron can undergo 180° deflection in the case of backscattering, its trajectory can be very complex. The maximum depth reached by an electron in the initial incident direction, called the range (or penetration depth), is less than its trajectory length.

The range (Rp) of an electron in a given medium depends on its energy and can be estimated by Equation II.7.

$$R_p = \int_{E_0}^{0} \frac{dE}{S_{total}(E)} \quad \textit{Equation II.7}$$

With E_0 the initial energy of the electron, S_{total} (E) is the total stopping power of the electron with energy E: $S_{total} = S_{col} + S_{rad}$. S_{col} and S_{rad} are the stopping power by collision and by radiation, respectively.

The range of an electron in matter depends on its initial energy and the density of the matter. For an electron beam, for example, averages that can be defined in various ways must be considered.

The mean range RM (Figure II.2) is the material thickness that reduces the percentage of electrons to half of its value in the absence of absorbing material, and the extrapolated range RC is the linear part at the end of the curve, marking an interaction point with the x-axis.

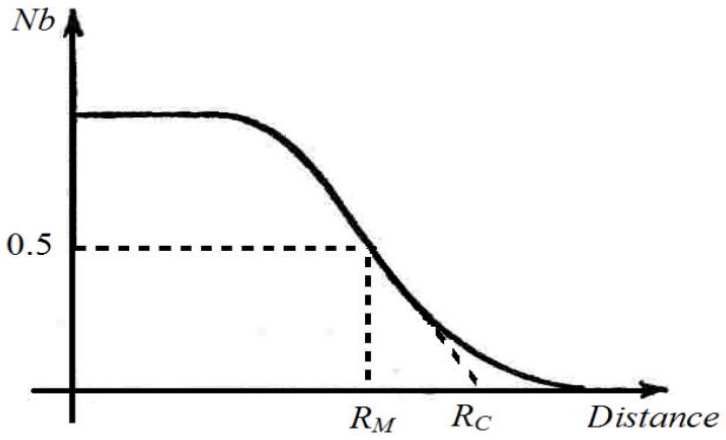

Figure II.2: Range and trajectory of an electron.

Table II.1: Stopping powers and ranges of electrons in water: values from NIST-ESTAR.

Kinetic Energy MeV	ESTAR STOPPING POWERS (MeV cm^2 /g)			
	Collision	Radiative	Total	D. effect parameter
1.000E-02	2.256E+01	3.898E-03	2.256E+01	0.000E+00
5.000E-02	6.603E+00	4.031E-03	6.607E+00	0.000E+00
1.000E-01	4.115E+00	4.228E-03	4.119E+00	0.000E+00
5.000E-01	2.034E+00	7.257E-03	2.041E+00	0.000E+00
1.000E+00	1.849E+00	1.280E-02	1.862E+00	2.428E-01
1.500E+00	1.822E+00	1.942E-02	1.841E+00	5.437E-01
2.000E+00	1.824E+00	2.678E-02	1.850E+00	8.218E-01
2.500E+00	1.834E+00	3.468E-02	1.868E+00	1.069E+00
3.000E+00	1.846E+00	4.299E-02	1.889E+00	1.288E+00
3.500E+00	1.858E+00	5.164E-02	1.910E+00	1.484E+00
4.000E+00	1.870E+00	6.058E-02	1.931E+00	1.660E+00
4.500E+00	1.882E+00	6.976E-02	1.951E+00	1.821E+00
5.000E+00	1.892E+00	7.917E-02	1.971E+00	1.967E+00

The range provides an estimate of the electron's trajectory length in matter. The heavier the material, the quicker the electron will be stopped. In the medical field, the density of soft tissues can be considered equivalent to that of water ($\rho = 1$). This is why the range of charged particles in water is important (see Figure II.1). Table II.1 presents the values of electron stopping powers in water for certain energies calculated according to the method defined by ICRU2 [ICRU-37, 1984].

II.1.3 THE GEANT4 SIMULATION CODE

GEANT4 is a free-to-use code (official site: http://geant4.web.cern.ch/geant4) for the complete and accurate simulation of particle transport through matter. Its application domains include high-energy physics, nuclear physics, and accelerator physics. GEANT4 allows users to integrate or modify physical models transparently and openly without disturbing the core architecture of the code.

It is supported by most computer platforms: SUN Solaris, Linux, MacOS with the gcc compiler, and Windows with a visual C++ compiler.

GEANT4 includes a comprehensive set of physical models describing the behavior of various particles in matter over a wide range of energies. These models have been compiled from data and expertise acquired over many years by physicists worldwide and from the experience gained from developing the earlier GEANT3 version. GEANT4 is also based on a model well-suited for tracking and interactions of particles in matter. All aspects of the simulation process are integrated into the code:

- System geometry;
- Involved materials;
- Fundamental particles involved;
- Primary event generation;
- Particle tracking through materials and electromagnetic fields;
- Response of sensitive detectors;
- Event storage;
- Visualization of detectors and particle trajectories;
- Analysis of simulation data.

Figure II.3 represents a minimal architecture of GEANT4 where the user implements their classes from the available base classes. Users can also build standalone applications or applications based on examples. Thanks to its flexibility and the variety of physical models it employs, GEANT4 is used in many medical applications today. GEANT4 is also one of the few codes allowing for microdosimetry, i.e., accurately tracking all particles and photons over distances of a few nanometers [Polf et al., 2014; Elbast et al., 2012].

Regarding particles and physical processes, several choices exist, but none are defined by default. Users must therefore target the needs of their simulation. After defining the particles involved in the simulation, each particle must be assigned the physical processes it may undergo and then choose the most appropriate physical model(s) for each process if necessary. We will now detail the electromagnetic processes in GEANT4 [Thiam, 2007]**.**

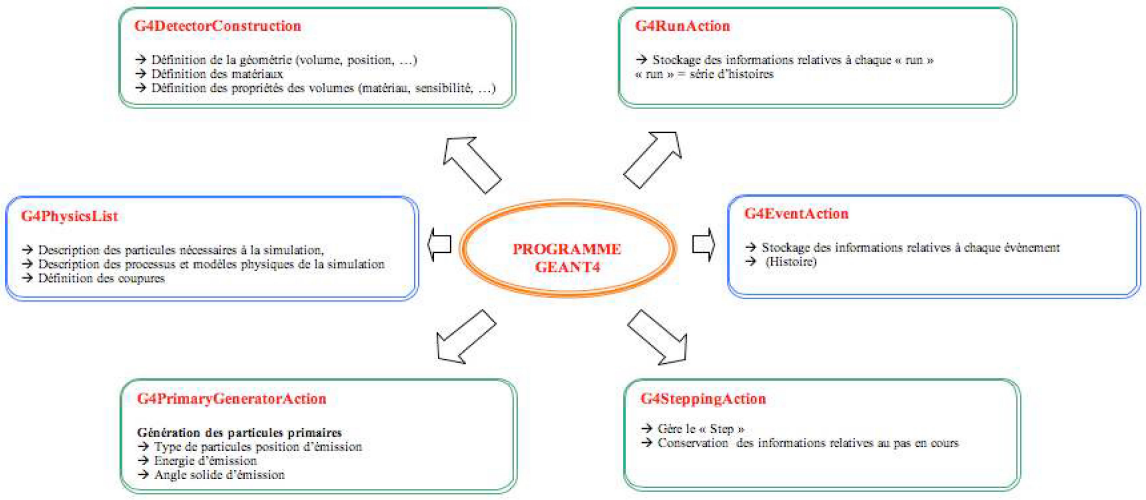

Figure II.3: Minimal architecture of a simulation code in GEANT4 [Thiam, 2007].

II.1.4 ELECTROMAGNETIC PROCESSES IN GEANT4

The electromagnetic process packages in GEANT4 (EM) manage the electromagnetic interactions of leptons, photons, hadrons, and ions. Three electromagnetic physics models using different libraries or databases of cross-sections are available in GEANT4: "Standard", "Low-energy", and "Penelope". Except for the fact that the ionization and bremsstrahlung processes for electrons are coupled, it is possible to choose the physical processes in these different models. The details are available in the regularly updated GEANT4 reference manual [GEANT4 PRM 2007]

The "Standard" model is applicable for an energy range of 10 keV to 100 TeV. All photon and electron interaction processes are included, except for Rayleigh scattering and atomic relaxation. Generally, the Standard model uses simple transport algorithms and is the most efficient and comprehensive.

The "Low-energy" model allows simulating particles down to 250 eV, which is especially necessary for medical applications, and it is defined solely from experimental data [Cullen et al. 1997; Perkins et al. 1997].

The "Penelope" model is based on the Monte Carlo PENELOPE code (version 2001). It is applicable for low or very low energies (ranging from a few eV up to 1 GeV). It simulates atomic relaxations related to the photoelectric effect, Compton scattering, and electron ionization. However, GEANT4 does not benefit from all the "sophisticated" particle transport mechanisms of the PENELOPE code. For example, mixed simulation [Baro et al. 1995] and random hinge algorithms [Bielajew et al. 1988] in electron transport are not modeled.

II.1.4.A PARTICLE TRACKING IN GEANT4

The tracking of particles through the various regions of the medium takes into account both geometric boundaries, interactions with matter, and the presence or absence of an electromagnetic field. In addition to the processes of ionization and Bremsstrahlung, the transport and its different stages are managed by the multiple scattering processes (MSC) in GEANT4, which we will discuss in more detail in the next section.

GEANT4 transports particles step by step. Each particle moves in steps, commonly referred to as "step." A step represents the smallest distance a particle can travel until its next interaction point. The step length is a random variable, determined based on the particle's energy at that step and the interaction cross-sections of the processes assigned to the particle. Interaction processes must therefore be assigned to each category of particle. Secondary particles emitted are generally tracked until they have deposited all their energy. However, for efficiency reasons, it is possible to discard secondary particles whose path is shorter than a user-defined value. This value is called a "cut" and can be expressed in length or energy. It has a direct influence on the energy deposition of the particle.

II.1.4.B THE MULTIPLE SCATTERING PROCESS "MSC-MULTIPLE SCATTERING" IN GEANT4

The MSC process (algorithm managing the "step" of electrons) in GEANT4 was developed by Urbán [Urbán, 2003], and it is applicable to all charged particles. This process is based on a correction of the "step" length at each stage of electron transport, which is then used to determine energy loss. If the end of the "step" length coincides with volume boundaries, lateral displacement may be partially ignored. A scattering angle is then used to determine the direction the electron takes in the next step during its transport. However, this scattering angle is not correlated with the correction of the "step" length and the lateral displacement of the electron. Unlike the EGSnrc code, the MSC process in GEANT4 does not account for spin effects and relativistic effects.

Geometric Boundaries

We have seen that electrons in GEANT4 are tracked "step" by "step." In principle, the "step" is defined by two points: the "Pre-step point" and the "Post-step point" (see Figure II.4).

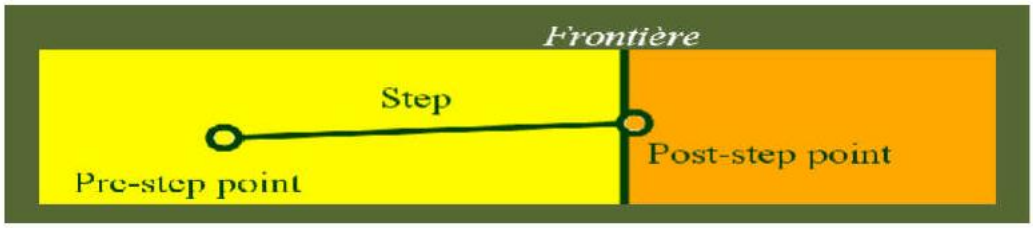

Figure II.4: Management of Geometric Boundaries in GEANT4.

The management of the "step" is therefore important as it takes into account several particle parameters (energy loss during the step, flight time spent per step, etc.). It thus conditions the distribution of energy within a given volume. When a particle reaches a geometric boundary, it is automatically stopped, and a portion of its energy is deposited at that point [Urbán, 2003; Thiam, 2007].

II.1.4.C LIMITATION OF STEPLENGTH FOR ELECTRONS

The step sizes of electrons are determined by locating the sites of each interaction while considering geometric boundaries. All electrons are tracked until their kinetic energies reach zero, unless a "cuts" threshold is set.

III. MATERIALS AND METHODS

III.1. THREE-DIMENSIONAL DISTRIBUTION

The Monte Carlo simulation was carried out with the geometry described in Figures III.2a) and III.2b), which show the following system: 188Re homogeneously distributed in a circular layer of cream with a diameter of 2 cm and a thickness of 1 mm, a protective layer of polystyrene (mylar) with a thickness of 10 µm.

The skin was simulated with a voxel-type mannequin whose dimensions were 2×2×0.1 cm^3, and a voxel size of 100 µm per side. The information about the chemical composition of the skin, air, and mylar, as well as the decay of 188Re, was extracted from the National Institute of Standards and Technology (NIST).

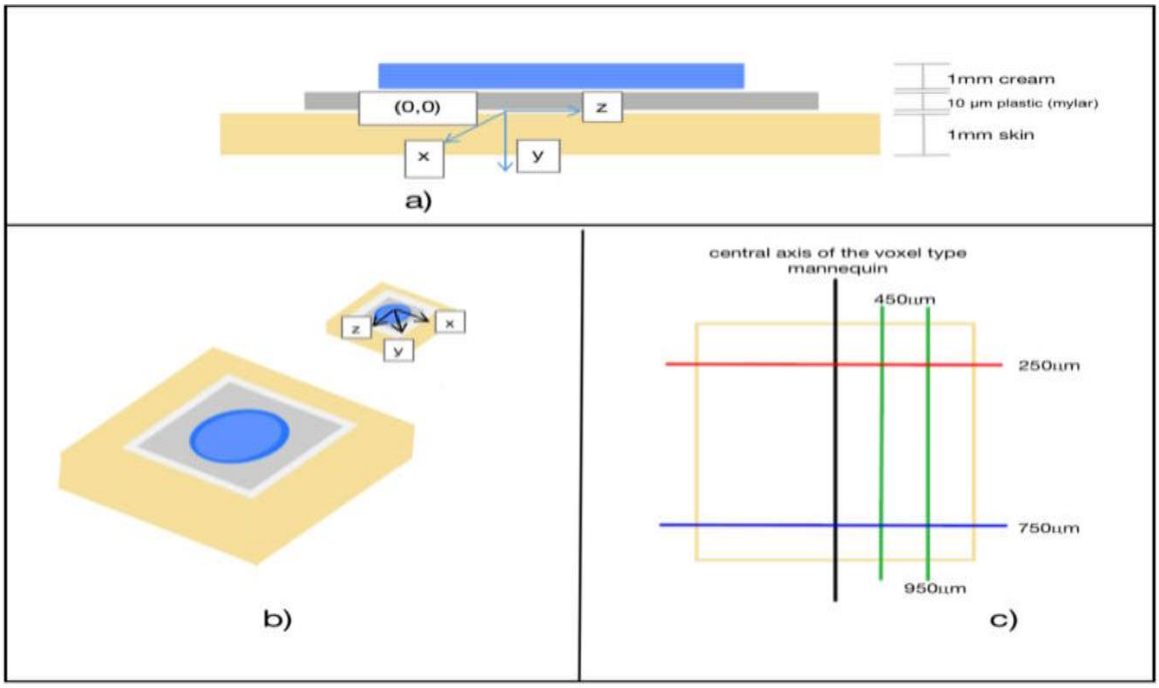

Figure III.1: (a) Sagittal view of the simulation scenario, (b) Isometric view of the simulation scenario, (c) Positions of the transverse (red and blue) and sagittal (green) cuts, the units are µm.

The geometry of the simulation was visually verified using GATE visualization. To validate the correct use of the GATE platform, previously reported results in Ec. (6) were replicated. The energy deposited per disintegration for each voxel in the geometry (MeV/Bq·s) was calculated, where eV =

electronvolt, Bq = Becquerel = (1 disintegration/second), s = second. A total of $5x10^8$ histories were simulated, and isodose surfaces and curves were plotted. The transverse and sagittal cuts are shown in Figure III.2c), which were made only in the voxelized mannequin representing the skin to describe the shape of the three-dimensional distribution of the absorbed dose through isodose curves. The origin (0,0,0) of the cuts made can be seen in the upper right corner of Figure III.2a).

III.2. THERAPEUTIC PROCEDURE

In clinical practice, the prescribed dose is an average of 50 Gy at a depth of 300-700 μm, based on previously conducted studies [Lee et al., 1997;Chung et al., 2000;2008;Pashazadeh et al., 2020;Cipriani et al., 2020]. Based on this, tables were generated with the required activity, depth, and irradiation time to meet this prescription. The procedure for calculating the treatment time was as follows:

1. The dose absorption kernel for each voxel was calculated using the following expression:
   KD (μBq·Gy·s−1) = EV (Bq·MeV·s−1) / 6.242×1012 (J·MeV−1) ***Equation III.1***
   Where KD is the dose kernel per voxel and EV is the energy deposited in each voxel.
2. The average dose kernel was calculated by considering all the voxels within the irradiated area at the prescribed depth.
3. The accumulated activity Â necessary to achieve the prescribed dose was calculated using the following equation:

$$\tilde{A} = \frac{50Gy}{KD} \qquad \textit{Equation III.2}$$

4. The treatment time was determined based on the initial activity in the cream and the accumulated activity required to reach the prescribed dose using Equation (III.3):

$$t_{trait} = -\frac{\ln\left(1-\frac{\lambda.\tilde{A}}{A_0}\right)}{\lambda_{Re}} \qquad \textit{Equation III.3}$$

Where $A_0$is the initial activity and λ_{Re} is the physical decay constant of 188Re.
Additionally, the homogeneity index (HI) was calculated, defined as follows:

$$HI = \frac{PDD_{min}}{PDD_{max}} \qquad \textit{Equation III.4}$$

Where PDD_{min} and PDD_{max} are the minimum and maximum percentages of dose in depth within the irradiated area.

CHAPTER IV: RESULTS AND DISCUSSION

IV.1. THREE-DIMENSIONAL DISTRIBUTION

The results in Fig. VI.3 show that the isodose surfaces approximately take the shape of a paraboloid. It is important to note that the radioactive source for the simulation is located at the top of the geometry, starting at z=1010 μm, as described in Fig. III.1.

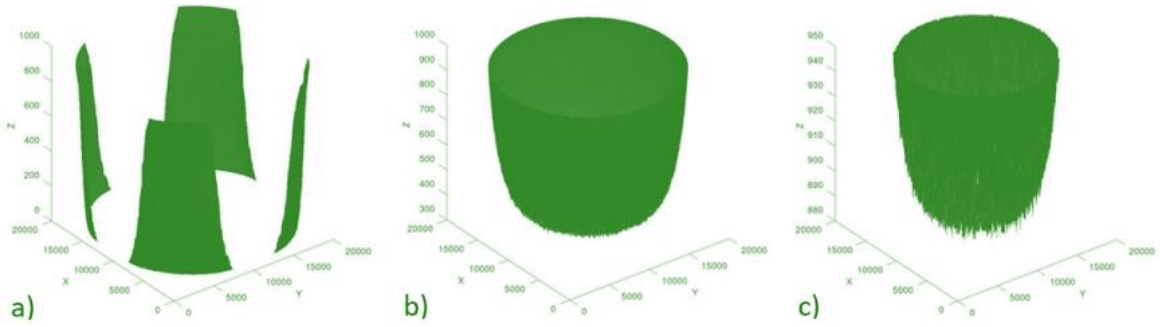

Figure IV.3: Isodose surfaces: a) 10%, b) 50%, and c) 90% of the maximum dose.

IV.1.1. TRANSVERSE CUTS

The distribution of the absorbed dose on the skin surface is described in Fig. VI.4a), where the shaded area represents the region receiving radiotherapy. It was found that the entire area on the surface is enclosed by the 40% isodose curve of the maximum dose, and the surrounding healthy region receives a maximum of 30%, while at a depth of 1.5 mm in healthy tissue, only 10% of the maximum dose is received. Figs. VI.4b) and VI.4c) present two axial cuts at 250 and 750 μm, which are the depths of interest in the BSR prescription. At a depth of 250 μm, the curve of the highest absorbed dose is 70% of the maximum dose, while at the edge of the area of interest, the isodose is 30%. In contrast to the absorbed dose on the surface and consistent with Fig.IV.3, which shows the spatial distribution of the absorbed dose, the 10% isodose at a transverse cut of 250 μm depth penetrates only 110 μm into healthy tissue. On the other hand, in the cut at 750 μm, the curve of the highest absorbed dose is 40% of the maximum dose, while at the edge of the area of interest, the isodose is 20%, and the 10% isodose penetrates only 63 μm into healthy tissue.

IV.1.2. SAGITTAL CUTS

From the sagittal cuts shown in Fig. III.1c), it is qualitatively demonstrated that the cuts at 50 µm and 450 µm from the longitudinal axis do not show a marked difference in the area covered by the isodose curves, as observed in Figs. IV.5a) and IV.5b), unlike the cut at 950 µm. In the sagittal cut at 50 µm, for a depth of 250 µm, the 70% curve covers the greatest length (Fig. IV.5a), similar to the sagittal cut at 450 µm. In the sagittal cut at 950 µm, only the curves from 40% to 10% are observed, which close abruptly. This indicates that at the periphery of the mannequin, the prescribed dose is not reached, so to cover the entire target volume, the radioactive source would have to be designed larger. Based on Fig. 5b), the source needs to extend 2.5 mm from the periphery of the target volume to achieve an average of 100% of the prescribed dose.

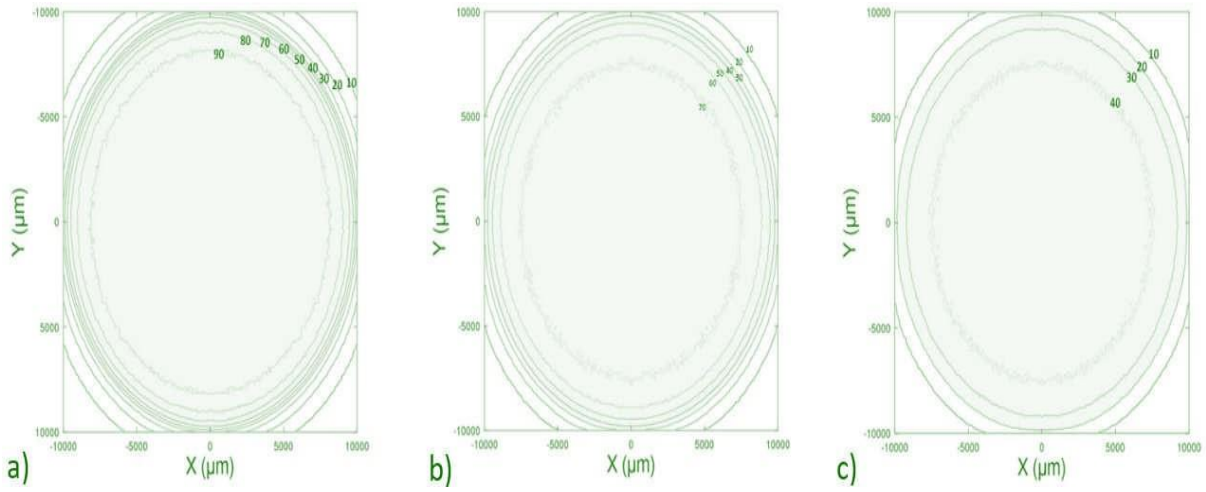

Figure IV.4: Isodose curves at depths of: a) 50 µm, b) 250 µm, and c) 750 µm.

It is worth mentioning that the study used a cylindrical geometry for the irradiated target volume, which allows for describing the behavior of the dose distribution at the periphery of the target volume.

This information is useful as it allows for understanding the amount of deposited energy and its distribution within the healthy tissue adjacent to the target area.

Based on this information, the shape and size of the radioactive source (cream with 188Re) can be determined to treat any area of squamous or basal cell cancer, regardless of the shape and size of the area to be treated, which is generally between 7 cm² and 10 cm² [Chung et al., 2000].

Based on Figs. IV.4 and IV.5, if the dose of 50 Gy is prescribed at a depth of 250 µm, the maximum absorbed dose outside the irradiated area in that cut is 22 Gy for the most superficial cut, and the dose outside the irradiated area is 29 Gy. Meanwhile, if the dose is prescribed for a depth of 750 µm, the maximum dose at the surface level is 51 Gy. According to the previous results, with the geometry defined in this work, it is possible to perform treatment with a prescription of 50 Gy for a depth of 250-650 µm, without exceeding the recommended dose limits for the epidermis. However, the absorbed dose to the epidermis is exceeded for a treatment at 750 µm.

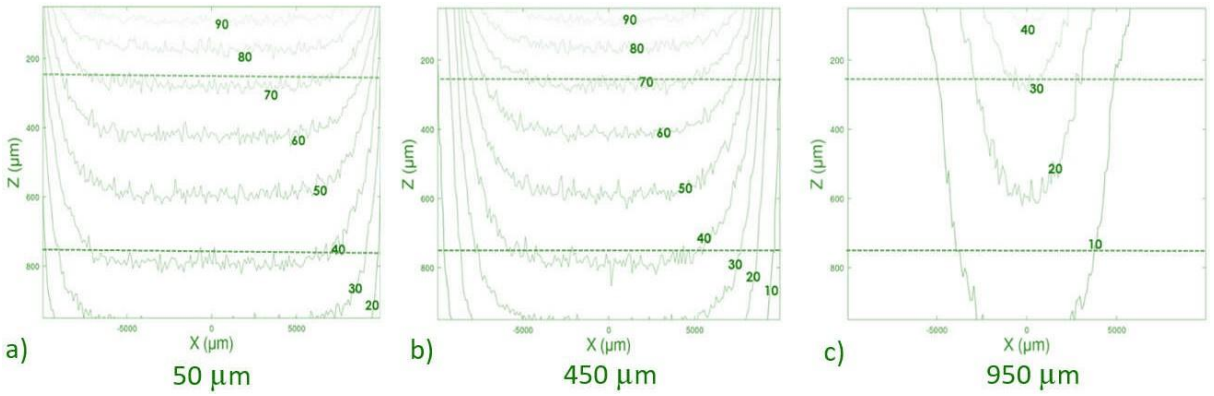

Figure IV.5: Isodose curves for the sagittal cut from the central axis to the periphery at a distanceof : a) 50 µm, b) 450 µm, and c) 950 µm. The blue and red dashed lines represent depths of 250 µm and 750 µm, respectively.

Table IV.1: The initial activity, irradiation time depending on the depth, radioactive concentration, and specific activity per area.

	Depth 250 µm	Depth 350 µm	Depth 450 µm	Depth 550 µm	Depth 650 µm	Depth 750 µm		
Initial activity (MBq)	Irradiation time (min)	Irradiation time (min)	Irradiation time (min)	Irradiation time (min)	Irradiation time (min)	Irradiation time (min)	Radioactive concentration (MBq/ml)	Specific radioactivity per area (MBq/cm²)
50	210	236	268	300	340	386	55	18
100	112	115	130	145	165	184	109	35
150	71	77	86	69	109	121	163	51
200	53.1	61	73.3	82.6	87.1	90.3	214.2	68.7
250	42	47	49	55	61	69	261.7	79.58
300	32	36	41	45	51	57	314.1	95.49
350	28	31	35	39	43	49	366.4	111.41
400	24	27	30	34	38	42	418.8	127.32
450	22	24	27	30	34	38	471.1	143.24
500	19	22	24	27	30	34	523.4	159.15

Most of the literature presents dose limitations for the skin considering conventional fractionation [Emami et al.,1991;Ginot et al.,2010]. In the case of BSR, the dose limit for the epidermis in a single session has been taken as a reference, with this limit being 45 Gy [Archambeau et al., 1995].

IV.2. THERAPEUTIC PROCEDURE

The obtained results are presented in Table IV.1, which includes the initial activity, irradiation time depending on the depth, radioactive concentration, and specific activity per area.

The results found are comparable to previous studies [Chung et al., 2000, Sedda et al., 2008. The irradiation time for clinical BSR ranges from 15 minutes to 2 hours, depending on the initial activity of 50 to 500 MBq as shown in the tabulated results.

Previous studies have reported the prescribed average dose only in the irradiated area [Lee et al., 1997;Sedda et al., 2008; De Paiva, 2023]. Some have been more specific, reporting the average dose on the skin surface above the tumor, throughout the tumor volume, and in the irradiated area [Chung et al., 2000; Cipriani et al., 2020]. From a more rigorous perspective and based on recommendations from ICRU reports [Ginot et al., 2010], it is not sufficient to report these parameters because they do not adequately express the homogeneity of the energy imparted to the target region. Given that the dose is prescribed over the irradiated area, it is appropriate to report homogeneity through the Homogeneity Index (HI), which was calculated using Eq. (4). The percentage of dose at maximum depth (PDD max) and minimum depth (PDD min) over the area defined by a slice at a given depth corresponds to the center and periphery of the irradiated area, respectively, as shown in Fig. IV.6.

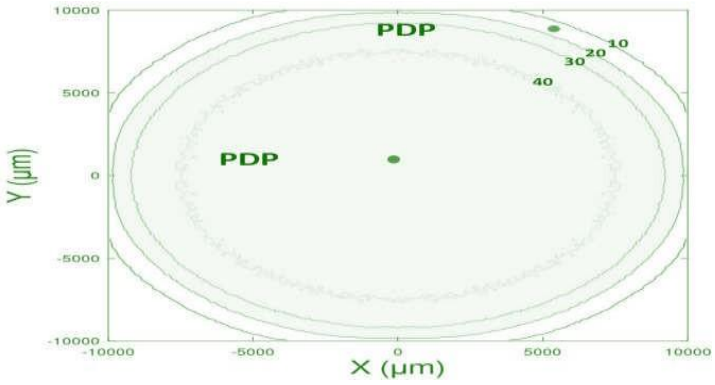

Figure IV.6: Representation of maximum and minimum PDD within a transverse cut. Theshaded part represents the irradiated area.

Table IV.2: Homogeneity Index (HI) for different depths.

Depth (μm)	250	350	450	550	650	750
HI	2.43	2.46	2.48	2.49	2.50	2.62

In case the area of interest is uniformly irradiated, HI=1, and as HI moves away from unity, there is less homogeneity over the irradiated area. Table IV.2 presents the calculated HI for the depths studied in this research. This aligns with Figures VI.4 and VI.5, but this Index quantitatively describes how homogeneity decreases as depth increases.

BSR is a treatment modality gradually being adopted as a viable and effective option for basal celland squamous cell carcinoma. Among its main characteristics are its simplicity of application, usually requiring only one session, adaptability to any surface, and effectiveness approaching 100% [Lee et al., 1997;Chung et al., 2000;Sedda et al.;2008;Pashazadeh et al., 2020;Cipriani et al., 2020], in addition to being completely painless.

A controversial aspect of BSR is the magnitude of the dose, as a single dose of 50 Gy is applied. In this regard, studies with kilovoltage photon therapies have shown that exceeding the 20 Gy thresholds is not advisable [Chan et al., 2007;McPartlin et al., 2014]. However, the distribution of absorbed dose given by kilovoltage photons and beta particles from 188Re is very different due to the difference in range between photons and betas. Therefore, additional studies are necessary to evaluate any dose limits for BSR to prevent harm to the treated patient.

The results shown in this work provide a quantitative description of the dose in the target and adjacent regions (healthy tissue), demonstrating that BSR is not only effective in treating basal and squamous cell carcinoma but also safe, as high doses are not delivered more than 2 mm into healthy tissue. Additionally, excellent cosmetic results have been reported in the majority of treated patients, who have also not reported post-treatment problems [Cipriani et al., 2020].

The three-dimensional Monte Carlo dosimetry of topical treatment for squamous and basal cell carcinoma with 188Re allowed describing and analyzing the behavior of the energy imparted throughout the volume of interest. This enabled calculating relevant aspects for BSR application, such as the maximum dose outside the irradiated area and the homogeneity of absorbed dose within the irradiation area, confirming that BSR is not only effective but also safe as long as there is no organ at risk within 2.5 mm of the irradiated area.

IV.4. CONCLUSION

Using the therapeutic configuration described in this work, which is employed in clinical practice, it is concluded that treatment depths from 250 to 650 μm can be achieved without exceeding the recommended absorbed dose limit for the epidermis. However, this limit is exceeded if the prescribed dose is reached at a depth of 750 μm.

This three-dimensional dosimetric analysis demonstrates that superficial brachytherapy with beta emissions from 188Re is an effective radiotherapy technique against squamous and basal cell carcinoma, safe for surrounding healthy tissue and overall patient well-being. It proves to be the most economical, safe, effective, practical, and painless radiotherapy technique, with excellent cosmetic outcomes post-treatment.

GENERAL CONCLUSION

In conclusion, the study demonstrates that superficial brachytherapy (SBT) with beta emissions from rhenium-188 (188Re) is an effective and safe treatment modality for both basal cell carcinoma(BCC) and squamous cell carcinoma (SCC). Utilizing three-dimensional Monte Carlo dosimetric analysis through the GATE (Geant4 Application for Tomographic Emission) simulation toolkit, the research provided detailed insights into the distribution of absorbed doses, confirming that 188Re SBT achieves high treatment efficacy while minimizing impact on surrounding healthy tissues. The GATE simulations showed precise dose distributions that conformed well to the target areas, with absorbed dose values meeting therapeutic requirements and ensuring minimal exposure to adjacent healthy tissues. These findings underscore the need for careful dose limit considerations, particularly concerning the proximity to critical organs.

Key advantages of 188Re SBT include its ability to conform to the irregular surfaces of skin lesions, providing high therapeutic efficacy with minimal cosmetic impact. The short half-life of 188Re ensures effective treatment with reduced radiation exposure to non-targeted areas, enhancing patient safety and comfort. The study highlighted the importance of precise dose calculation and delivery to optimize treatment outcomes and minimize potential side effects. The versatility of 188Re SBT in treating various sizes and locations of skin cancers further underscores its potential as a practical and patient-friendly treatment modality. The technique's simplicity, adaptability to various surfaces, and high cosmetic outcomes reinforce its practicality and patient acceptance.

Future research should aim to refine dose delivery techniques and explore combination therapies that could further enhance the effectiveness of 188Re SBT. Clinical trials involving larger patient populations and long-term follow-up are necessary to fully establish the efficacy and safety profile of this treatment. Additionally, investigating the use of 188Re SBT in other superficial cancers could broaden its therapeutic applications.

In summary, 188Re-based superficial brachytherapy represents a significant advancement in the treatment of non-melanoma skin cancers, offering a combination of high efficacy, safety, and excellent cosmetic outcomes. This novel approach holds great promise for improving the management of skin cancer and enhancing the overall quality of life for patients. The obtained results with GATE provide a robust foundation for the clinical implementation of this technique, supporting its potential to become a standard therapy for superficial skin cancers.

BIBLIOGRAPHY

1. Leiter, U., Keim, U., & Garbe, C. (2020). Epidemiology of Skin Cancer: Update 2019. In Advances in Experimental Medicine and Biology (pp. 123–139). https://doi.org/10.1007/978-3-030-46227-7_6

2. Hasan, N., Nadaf, A., Imran, M., Jiba, U., Sheikh, A., Almalki, W. H., Almujri, S. S., Mohammed, Y., Kesharwani, P., & Ahmad, F. J. (2023). Skin cancer: understanding the journey of transformation from conventional to advanced treatment approaches. Molecular Cancer, 22(1). https://doi.org/10.1186/s12943-023-01854-3

3.Yélamos, O., Geller, S., & Tokez, S. (2023). Skin cancer special issue in Skin Health and Disease. Skin Health and Disease, 3(2). https://doi.org/10.1002/ski2.224

4.Simões, M. C. F., Sousa, J. J. S., & Pais, A. A. C. C. (2015). Skin cancer and new treatment perspectives: A review. In Cancer Letters (Vol. 357, Issue 1, pp. 8–42). Elsevier Ireland Ltd. https://doi.org/10.1016/j.canlet.2014.11.001

5.Naik, P. P. (2021). Cutaneous Malignant Melanoma: A Review of Early Diagnosis and Management. World Journal of Oncology, 12(1), 7–19. https://doi.org/10.14740/wjon1349

6.Orzan OA, Çandru A, Jecan CR. Controversies in the diagnosis and treatment of early cutaneous melanoma. J Med Life. 2015 Apr-Jun;8(2):132-41. PMID: 25866567; PMCID: PMC4392104.

7.Berwick, M., & Garcia, A. (2020). Solar UV Exposure and Mortality from Skin Tumors: An Update. In Advances in experimental medicine and biology (Print) (pp. 143–154). https://doi.org/10.1007/978-3-030-46227-7_7

8.Dika, E., Scarfì, F., Ferracin, M., Broseghini, E., Marcelli, E., Bortolani, B., Campione, E., Riefolo, M., Ricci, C., & Lambertini, M. (2020). Basal cell carcinoma: A Comprehensive review. International Journal of Molecular Sciences (Online), 21(15), 5572. https://doi.org/10.3390/ijms21155572

9.Linares, M. a. G., Zakaria, A. A., & Nizran, P. (2015). Skin cancer. Primary Care, 42(4), 645–659. https://doi.org/10.1016/j.pop.2015.07.006

10.Corchado-Cobos, R., García-Sancha, N., González-Sarmiento, R., Pérez-Losada, J., & Cañueto, J. (2020). Cutaneous squamous cell carcinoma: From biology to therapy. International Journal of Molecular Sciences, 21(8), 2956. https://doi.org/10.3390/ijms21082956

11.Badash, I., Shauly, O., Lui, C., Gould, D. J., & Patel, K. M. (2019). Nonmelanoma Facial skin Cancer: A review of diagnostic strategies, surgical treatment, and reconstructive techniques. Clinical Medicine Insights. Ear, Nose and Throat, 12, 117955061986527. https://doi.org/10.1177/1179550619865278

12.Anthony, M. L. (2000). Surgical treatment of nonmelanoma skin cancer. AORN Journal, 71(3), 550–564. https://doi.org/10.1016/s0001-2092(06)61577-9

13.Prickett KA, Ramsey ML. Mohs Micrographic Surgery. [Updated 2023 Jul 25]. In: StatPearls [Internet]. Treasure Island (FL): StatPearls Publishing; 2024 Jan-. Available from: https://www.ncbi.nlm.nih.gov/books/NBK441833

14.Fournier, S., Laroche, A., Leblanc, M., Bourgeault, E., Singbo, M. N. U., Turcotte, S., Blouin, M., & Alain, J. (2020). Prospective clinical trial comparing curettage and cryosurgery to curettage and electrodesiccation in the management of minimally invasive basal and squamous cell carcinomas. Journal of Cutaneous Medicine and Surgery, 24(6), 596–600. https://doi.org/10.1177/1203475420943258

15.Castellucci, P., Savoia, F., Farina, A., Lima, G. M., Patrizi, A., Baraldi, C., Zagni, F., Vichi, S., Pettinato, C., Morganti, A. G., Strigari, L., & Fanti, S. (2021). High dose brachytherapy with non sealed 188Re (rhenium) resin in patients with non-melanoma skin cancers (NMSCs): single center preliminary results. European Journal of Nuclear Medicine and Molecular Imaging, 48(5), 1511–1521. https://doi.org/10.1007/s00259-020-05088-z

16.Correia JH, Rodrigues JA, Pimenta S, Dong T, Yang Z. Photodynamic Therapy Review: Principles, Photosensitizers, Applications, and Future Directions. Pharmaceutics. 2021 Aug 25;13(9):1332. doi: 10.3390/pharmaceutics13091332. PMID: 34575408; PMCID: PMC8470722.

17.Pustinsky I, Dvornikov A, Kiva E, Chulkova S, Egorova A, Gladilina I, Peterson S, Lepkova N, Grishchenko N, Galaeva Z, Baisova A, Kalinin S. Cryosurgery for Basal Cell Skin Cancer of the Head: 15 Years of Experience. Life (Basel). 2023 Nov 20;13(11):2231. doi: 10.3390/life13112231. PMID: 38004371; PMCID: PMC10671957.

18.Garbutcheon-Singh, K. B., & Veness, M. J. (2019). The role of radiotherapy in the management of non-melanoma skin cancer. Australasian Journal of Dermatology. doi:10.1111/ajd.13025

19.Locke, J., Karimpour, S., Young, G., Lockett, M. A., & Perez, C. A. (2001). Radiotherapy for epithelial skin cancer. International Journal of Radiation Oncology, Biology, Physics, 51(3), 748–755. https://doi.org/10.1016/s0360-3016(01)01656-x

20.McGregor S, Minni J, Herold D. Superficial Radiation Therapy for the Treatment of Nonmelanoma Skin Cancers. J Clin Aesthet Dermatol. 2015 Dec;8(12):12-4. PMID: 26705443; PMCID: PMC4689506.

21.Yosefof E, Kurman N, Yaniv D. The Role of Radiation Therapy in the Treatment of Non-Melanoma Skin Cancer. Cancers (Basel). 2023 Apr 22;15(9):2408. doi: 10.3390/cancers15092408. PMID: 37173875; PMCID: PMC10177122.

22.Skowronek, J. (2015). Brachytherapy in the treatment of skin cancer: An overview. In Postepy Dermatologii i Alergologii (Vol. 32, Issue 5, pp. 362–367). Termedia Publishing House Ltd. https://doi.org/10.5114/pdia.2015.54746

23.Zaorsky, N. G., Lee, C. T., Zhang, E., Keith, S. W., & Galloway, T. J. (2017). Hypofractionated radiation therapy for basal and squamous cell skin cancer: A meta-analysis. Radiotherapy and Oncology, 125(1), 13–20. https://doi.org/10.1016/j.radonc.2017.08.011

24.Kopera, D. (2021). Citation for this article: Daisy Kopera. Prevention of Actinic Keratosis with Topical Imiquimod 3.75% Cream. In Cancer Prev ention : Current Research Journal (Vol. 4, Issue 1).

25.Gracia-Cazaña, T., González, S., & Gilaberte, Y. (2016). Resistance of nonmelanoma skin cancer to nonsurgical treatments. Part I: Topical treatments. Actas Dermo-sifiliográficas/Actas Dermo-sifiliográFicas, 107(9), 730–739. https://doi.org/10.1016/j.adengl.2016.08.016

26.Gross, K., Kircik, L., & Kricorian, G. (2007). 5% 5-Fluorouracil cream for the treatment of small superficial basal cell carcinoma: efficacy, tolerability, cosmetic outcome, and patient satisfaction. Dermatologic Surgery, 33(4), 433–440. https://doi.org/10.1111/j.1524-4725.2007.33090.x

27.Cullen, J. K., Simmons, J. L., Parsons, P. G., & Boyle, G. M. (2020). Topical treatments for skin cancer. Advanced Drug Delivery Reviews, 153, 54–64. https://doi.org/10.1016/j.addr.2019.11.002

28.Sahu, P., Kashaw, S. K., Sau, S., Kushwah, V., Jain, S., Agrawal, R. K., & Iyer, A. K. (2019). PH responsive 5-Fluorouracil loaded biocompatible nanogels for topical chemotherapy of aggressive melanoma. Colloids and Surfaces. B, Biointerfaces, 174, 232–245. https://doi.org/10.1016/j.colsurfb.2018.11.018

29.Cipriani, C., Desantis, M., Dahlhoff, G., Brown, S. D., Wendler, T., Olmeda, M., Pietsch, G., & Eberlein, B. (2020). Personalized irradiation therapy for NMSC by rhenium-188 skin cancer therapy: a long-term retrospective study. Journal of Dermatological Treatment, 1–7. https://doi.org/10.1080/09546634.2020.1793890

30.Lepareur, N., Lacœuille, F., Bouvry, C., Hindré, F., Garcion, E., Chérel, M., Noiret, N., Garin, E., & Knapp, F. F. R. (2019). Rhenium-188 labeled Radiopharmaceuticals: Current clinical applications in oncology and Promising Perspectives. Frontiers in Medicine, 6. https://doi.org/10.3389/fmed.2019.00132

31.Pillai, M. R., Dash, A., & Knapp, F. F. (2012). Rhenium-188: Availability from the 188W/188Re Generator and Status of Current Applications. Current Radiopharmaceuticals, 5(3), 228–243. https://doi.org/10.2174/1874471011205030228

32.Jeong, J. M., Lee, Y. J., Kim, E. H., Chang, Y. S., Kim, Y. J., Son, M., Lee, D. S., Chung, J. K., & Lee, M. C. (2003). Preparation of 188Re-labeled paper for treating skin cancer. Applied Radiation and Isotopes, 58(5), 551–555. https://doi.org/10.1016/S0969-8043(03)00063-0

33.Rodriguez-Herklotz, W., Torres-Garcia, E., Ferro-Flores, G., Isaac-Olive, K., & Aranda-Lara, L. (2022). Dosimetría tridimensional por Monte Carlo del tratamiento tópico con 188Re de carcinoma

de células escamosas y basales. Revista Mexicana de Fisica, 68(4). https://doi.org/10.31349/RevMexFis.68.041101

34.National Research Council (US) Committee on Evaluation of EPA Guidelines for Exposure to Naturally Occurring Radioactive Materials. Evaluation of Guidelines for Exposures to Technologically Enhanced Naturally Occurring Radioactive Materials. Washington (DC): National Academies Press (US); 1999. Appendix, Radiation Quantities and Units, Definitions, Acronyms. Available from: https://www.ncbi.nlm.nih.gov/books/NBK230653/

35.Chung, Y. L., Lee, J. D., Bang, D., Lee, J. B., Park, K. B., & Lee, M. (2000). Treatment of Bowen's disease with a specially designed radioactive skin patch. European Journal of Nuclear Medicine and Molecular Imaging, 27(7), 842–846. https://doi.org/10.1007/s002590000262

36.Lee JD, Park KK, Lee MG, Kim EH, Rhim KJ, Lee JT, Yoo HS, Kim YM, Park KB, Kim JR. Radionuclide therapy of skin cancers and Bowen's disease using a specially designed skin patch. J Nucl Med. 1997 May;38(5):697-702. PMID: 9170430.

37.Sedda, A. F., Rossi, G., Cipriani, C., Carrozzo, A. M., & Donati, P. (2008). Dermatological high-dose-rate brachytherapy for the treatment of basal and squamous cell carcinoma. Clinical and Experimental Dermatology, 33(6), 745–749. https://doi.org/10.1111/j.1365-2230.2008.02852.x

38.Pashazadeh, A., Robatjazi, M., Castro, N. J., & Friebe, M. (2020). A multiwell applicator for conformal brachytherapy of superficial skin tumors: A simulation study. Skin Research and Technology, 26(4), 537–541. https://doi.org/10.1111/srt.12826

39.Ginot, A., Doyen, J., Hannoun-Lévi, J., & Courdi, A. (2010). Dose de tolérance des tissus sains : la peau et les phanères. Cancer/Radiothérapie/Cancer Radiothérapie, 14(4–5), 379–385. https://doi.org/10.1016/j.canrad.2010.03.015

40.Emami, B., Lyman, J., Brown, A., Cola, L., Goitein, M., Munzenrider, J., Shank, B., Solin, L., & Wesson, M. (1991). Tolerance of normal tissue to therapeutic irradiation. International Journal of Radiation Oncology, Biology, Physics, 21(1), 109–122. https://doi.org/10.1016/0360-3016(91)90171-y

41.Archambeau, J. O., Pezner, R., & Wasserman, T. (1995). Pathophysiology of irradiated skin and breast. International Journal of Radiation Oncology, Biology, Physics, 31(5), 1171–1185. https://doi.org/10.1016/0360-3016(94)00423-i

42.Chan, S., Dhadda, A., & Swindell, R. (2007). Single fraction radiotherapy for small superficial carcinoma of the skin. Clinical Oncology, 19(4), 256–259. https://doi.org/10.1016/j.clon.2007.02.004

43.McPartlin, A. J., Slevin, N. J., Sykes, A. J., & Rembielak, A. (2014). Radiotherapy treatment of non-melanoma skin cancer: a survey of current UK practice and commentary. ˜the œBritish Journal of Radiology/British Journal of Radiology, 87(1043), 20140501. https://doi.org/10.1259/bjr.20140501

44.Thiam, C. O. (2007). "Dosimétrie en radiothérapie et curiethérapiepar simulation MonteCarlo GATE sur grille informatique." Manuscrit de thèse

45.Jan, S., Santin, G., Strul, D., Staelens, S., Assié, K., Autret, D., Avner, S., Barbier, R., Bardiès, M., Bloomfield, P. M., Brasse, D., Breton, V., Bruyndonckx, P., Buvat, I., Chatziioannou, A. F., Choi, Y., Chung, Y. H., Comtat, C., Donnarieix, D., . . . Morel, C. (2004). GATE: a simulation toolkit for PET and SPECT. *Physics in Medicine & Biology/Physics in Medicine and Biology*, *49*(19), 4543–4561. https://doi.org/10.1088/0031-9155/49/19/007

46.Sarrut, D., Bardiès, M., Boussion, N., Freud, N., Jan, S., Létang, J., Loudos, G., Maigne, L., Marcatili, S., Mauxion, T., Papadimitroulas, P., Perrot, Y., Pietrzyk, U., Robert, C., Schaart, D. R., Visvikis, D., & Buvat, I. (2014). A review of the use and potential of the GATE Monte Carlo simulation code for radiation therapy and dosimetry applications. *Medical Physics on CD-ROM/Medical Physics*, *41*(6Part1), 064301. https://doi.org/10.1118/1.4871617

47.Maigne, L. (n.d.). Dosimétrie personnalisée par simulation Monte Carlo GATE sur grille de calcul. Application à la curiethérapie oculaire. https://theses.hal.science/tel-00011404

48. [ICRU-37, 1984] ICRU (International Commision on Radiation Units and Measurements)(1984) ICRU Repport 37 : Stopping Powers for Electrons and Positrons; ICRU Report n◦37 (Bethesda M.D., ICRU).

49.Polf, J. C., Mackin, D., Lee, E., Avery, S., & Beddar, S. (2014). Detecting prompt gamma emission during proton therapy: the effects of detector size and distance from the patient. *Physics in Medicine & Biology/Physics in Medicine and Biology*, *59*(9), 2325–2340. https://doi.org/10.1088/0031-9155/59/9/2325

50.Elbast, M., Saudo, A., Franck, D., Petitot, F., & Desbrée, A. (2011). Microdosimetry of alpha particles for simple and 3D voxelised geometries using MCNPX and Geant4 Monte Carlo codes. *Radiation Protection Dosimetry*, *150*(3), 342–349. https://doi.org/10.1093/rpd/ncr401

51.Cullen, D. E., Hubbell, J. H., & Kissel, L. (1997). *EPDL97: the evaluated photo data library `97 version*. https://doi.org/10.2172/295438

52.Baró, J., Sempau, J., Fernández-Varea, J., & Salvat, F. (1995). PENELOPE: An algorithm for Monte Carlo simulation of the penetration and energy loss of electrons and positrons in matter. *Nuclear Instruments and Methods in Physics Research. Section B, Beam Interactions With Materials and Atoms/Nuclear Instruments & Methods in Physics Research. Section B, Beam Interactions With Materials and Atoms*, *100*(1), 31–46. https://doi.org/10.1016/0168-583x(95)00349-5

53.Perkins S.T., et al.. (1997) Tables and graphs of atomic sub-shell and relaxation data derived from the LLNL Evaluated Atomic Data Library (EADL), Z=1- 100, UCRL-50400 30 1997.

54.Urbán L. (2003) MSC angular distributions in GEANT4 - where we are now ? RMKI Research Institute for Particle and Nuclear Physics, H-1525 Budapest, P.O. Box 49, Hungary and CERN, CH-1211 Geneva 23, Switzerland.

54.Bielajew A.F. and Rogers D.W.O. (1988) Variance reduction techniques, Monte-Carlo Transport of Electrons and Photons, edition T.M. Jenkins, W.R. Nelson and A. Rindi, New York : Plenum : 407-20.

55.M. Laoues, R. Khelifi and A.Sidi Moussa: Validation of the Monte Carlo GATE platform for the dosimetry of ocular protontherapy. InternationalConference on Monte Carlo Techniques for Medical Applications (MCMA)/ Book of abstracts, Page 13-19,2017.